

## Supplementary Information

---

### Silicon Microfabricated Reactor for *Operando* XAS/DRIFTS Studies of Heterogeneous Catalytic Reactions

B. Venezia<sup>1†</sup>, E. Cao<sup>1†</sup>, S. K. Matam<sup>2,3</sup>, C. Waldron<sup>1</sup>, G. Cibir<sup>4</sup>, E. K. Gibson<sup>2,5</sup>, S. Golunski<sup>3</sup>,  
P. P. Wells<sup>2,6</sup>, I. Silverwood<sup>7</sup>, C. R. A. Catlow<sup>2,3,8</sup>, G. Sankar<sup>8</sup>, A. Gavriilidis<sup>1\*</sup>

<sup>1</sup>*Department of Chemical Engineering, University College London, London WC1E 7JE, UK*

<sup>2</sup>*The UK Catalysis Hub, Research Complex at Harwell, Harwell OX11 0FA, UK*

<sup>3</sup>*Cardiff Catalysis Institute, School of Chemistry, Cardiff University, Cardiff CF10 3AT, UK*

<sup>4</sup>*Diamond Light Source Ltd., Harwell Science and Innovation Campus, Didcot OX11 0DE, United Kingdom*

<sup>5</sup>*School of Chemistry, The University of Glasgow, Glasgow G12 8QQ, UK*

<sup>6</sup>*School of Chemistry, University of Southampton, Southampton SO17 1BJ, UK*

<sup>7</sup>*ISIS Pulsed Neutron and Muon Facility, Science and Technology Facilities Council, Rutherford Appleton  
Laboratory, Harwell Science and Innovation Campus, Oxon, UK*

<sup>8</sup>*Department of Chemistry, University College London, London WC1H 0AJ, UK*

† These authors contributed equally

\*corresponding author: [a.gavriilidis@ucl.ac.uk](mailto:a.gavriilidis@ucl.ac.uk)

## Contents

Microfabricated silicon-glass reactor and microreactor assembly.....	2
Schematic of the experimental rig.....	3
Linear combination fitting.....	4
Axial dispersion in the micropacked-bed.....	5
External and internal mass transfer.....	7
References .....	9

## Microfabricated silicon-glass reactor and microreactor assembly

Pictures of the silicon-glass microreactor are presented in Figure S1. It is possible to observe in the top pictures of both the back and the front side, the thermocouple wells used to insert the thermocouples and the larger X-ray slits, through which X-ray beams were focussed. The DRIFTS window is visible on the front side, while the back side shows the catalyst bed with silica beads.

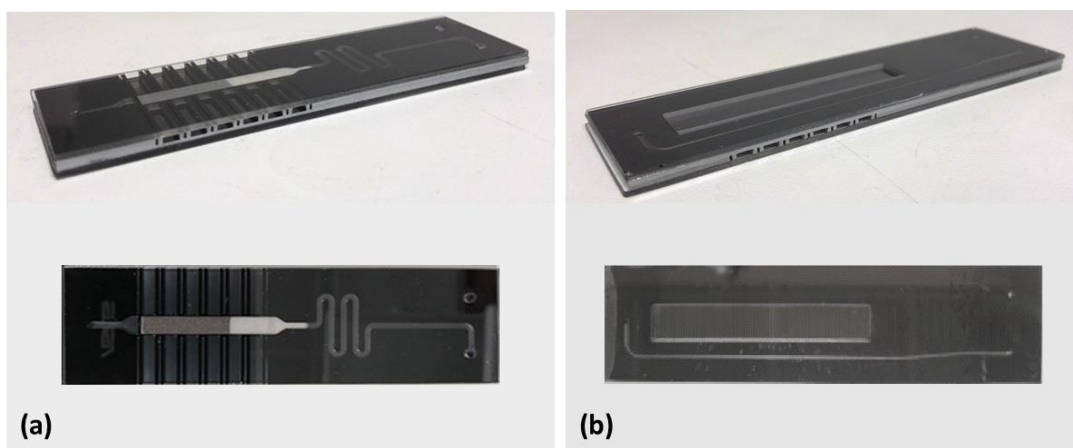


**Figure S1.** Pictures of the silicon-glass microreactor: (a) back side and (b) front side

Figure S2 shows the microreactor in an in-house made heating unit. This comprised of a ceramic heater which was fitted into a stainless steel holder.

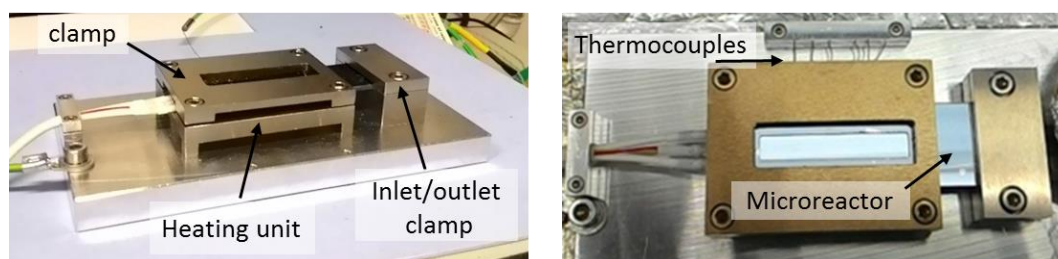


**Figure S2.** Microreactor assembly consisting of a ceramic heating unit, a clamping system to hold it in place and thermocouples on the side to measure the temperature profile.

## Schematic of the experimental rig

The experimental rig used for the *operando* XAS and DRIFTS studies is presented in Figure S3. CH<sub>4</sub>/He was used for the *operando* XAS during methane combustion over 2 wt% Pd/Al<sub>2</sub>O<sub>3</sub>, while CO/He was employed for the *operando* DRIFTS during CO oxidation over 1 wt% Pt/Al<sub>2</sub>O<sub>3</sub>.

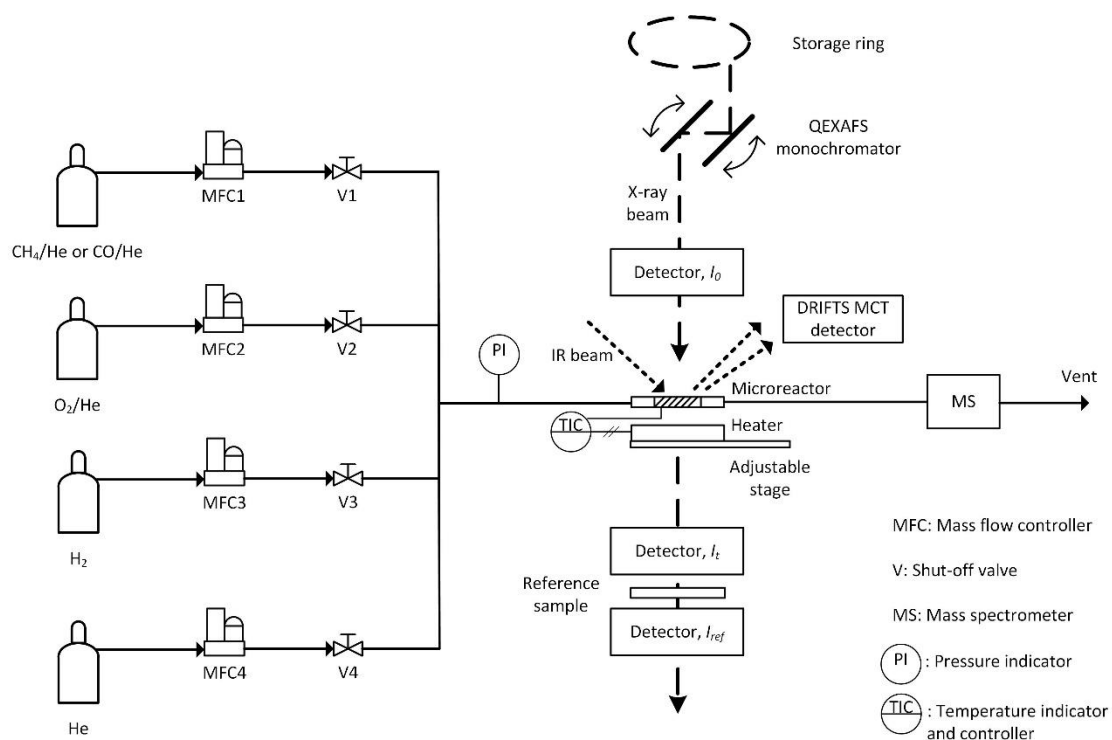


**Figure S3.** Schematic representation of the *operando* XAS/MS and DRIFTS/MS experimental setup. Note that in this work the XAS/MS and DRIFTS/MS experiments were performed separately.

## Linear combination fitting

An example of a linear combination fit (LCF) of a XANES spectrum for the catalyst at 250 °C is presented in Figure S4. The fitting was performed with 0.923 and 0.077 weightings for PdO and Pd<sup>0</sup> reference spectra respectively, which led to an *R*-factor of 0.00016 and a visibly small residual.

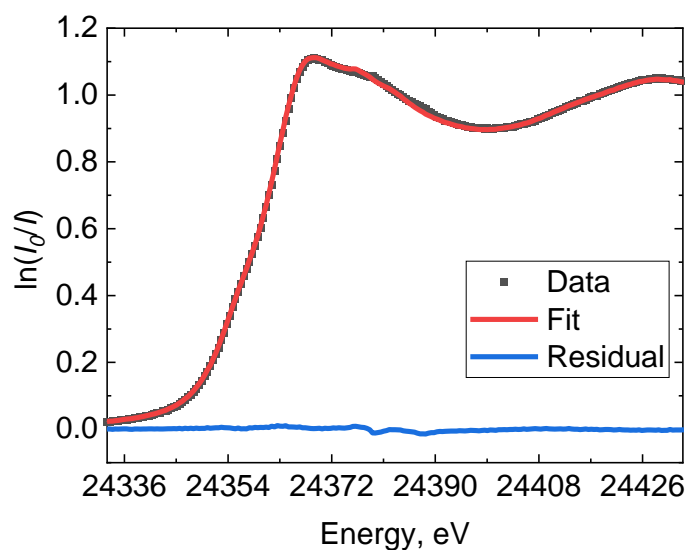


**Figure S4.** Representative LCF (red line) of the experimental XANES data (black dots) and resulting residual (blue line) for the 2 wt% Pd/Al<sub>2</sub>O<sub>3</sub> catalyst at the inlet of the catalyst bed at 250 °C. Experimental details can be found in section 2.3 of the main paper.

## Axial dispersion in the micropacked-bed

The dispersion in packed-bed tubular reactors is a function of the flow regime and the fluid physical properties [1]. The former is generally characterised by the particle Reynolds number ( $Re_p$ ), while the latter is described by the Schmidt number ( $Sc$ ), defined in Eq. (S1) and Eq. (S2), respectively.

$$Re_p = \frac{u \rho d_p}{\mu} \quad (S1)$$

$$Sc = \frac{\mu}{\rho D_m} \quad (S2)$$

These dimensionless numbers are calculated considering the catalyst particle diameter ( $d_p$ ), the free-stream superficial velocity ( $u$ ), the density ( $\rho$ ), the molecular diffusivity ( $D_m$ ) and the dynamic viscosity of the fluid ( $\mu$ ). The density of the gas, assumed to be made of helium only, can be calculated using the ideal gas law (Eq. (S3)), where  $p$  is the total pressure (1 atm),  $MM_{He}$  is the helium molar mass (4 kg/kmol),  $R$  the ideal gas constant (8.3145 J/mol/K) and  $T$  the absolute temperature (673.15 K).

$$\rho = \frac{p MM_{He}}{RT} \quad (S3)$$

The molecular diffusivity of methane in helium is reported by Cussler at 298 K and atmospheric pressure and it is equal to 0.675 cm<sup>2</sup>/s [2]. To calculate the molecular diffusivity of methane in helium at 673.15 K, Eq. (S4) can be used, which relates the molecular diffusivity for a bulk gas to the change in absolute temperature at constant pressure [3].

$$D_m(T_2) = D_m(T_1) \left( \frac{T_2}{T_1} \right)^{1.75} \quad (S4)$$

Finally, the viscosity of the gas (assumed to be helium) at 400 °C (673.15 K) can be calculated according to Eq. (S5), as reported by Kestin and Leidenfrost [4].

$$\mu_{He}(\mu P) = 5.023 T(K)^{0.647} \quad (S5)$$

Table S1 reports the dimensions of the reactor, while Table S2 shows the fluid and physical properties of the reacting 1 % CH<sub>4</sub>/He and 4 % O<sub>2</sub>/He at 40 NmL/min and 400 °C, including  $Re_p$  and  $Sc$ .

**Table S1.** Catalyst bed dimensions in the silicon-glass microreactor.

Property	Value
Width ( $W$ ), m	$3 \cdot 10^{-3}$
Depth ( $D$ ), m	$600 \cdot 10^{-6}$
Length ( $L_b$ ), m	$15 \cdot 10^{-3}$
Empty cross sectional area, m <sup>2</sup>	$1.8 \cdot 10^{-6}$
Empty volume ( $V_r$ ), m <sup>3</sup>	$0.027 \cdot 10^{-6}$

**Table S2.** Fluid dynamic and catalyst physical properties for 1 % CH<sub>4</sub>/He and 4 % O<sub>2</sub>/He at 400 °C.

Property	Value
$d_p$ , μm	60
$v$ , NmL/min	40
$u$ , m/s	0.37
$\rho$ , kg/m <sup>3</sup>	0.072
$D_m$ , m <sup>2</sup> /s	$2.81 \cdot 10^{-4}$
$\mu$ , mPa·s	0.034
$Re_p$	0.047
$Sc$	1.71

Generally, the axial dispersion coefficient ( $D_{ax}$ ) is described by the dimensionless Péclet number ( $Pe$ ), which, in the case of packed-bed reactors, is calculated from the particle Péclet number ( $Pe_p$ ), the particle diameter and the catalyst bed length ( $L_b$ ) (Eq. (S6)) [5]. The  $Pe_p$  is related to the  $Re_p$  and  $Sc$  according to Eq. (S7), where  $\varphi$  is the catalyst bed porosity (assumed to be 0.4) [3] and  $\tau$  is the catalyst bed tortuosity (assumed to be 1.4) [6]. Eq. (S7) is valid for a ratio between the reactor diameter and particle size ( $d_p$ ) larger than 15 and a ratio between catalyst bed length ( $L_b$ ) and reactor diameter larger than 20 [6]. In our work, the ratio between the catalyst bed length and the microchannel depth ( $L_b/D$ ) is 25, but since the cross section is rectangular,  $D/d_p$  is 10 and  $W/d_p$  is 50.

$$Pe = \frac{u L_b}{D_{ax}} = Pe_p \frac{L_b}{d_p} \quad (S6)$$

$$\frac{1}{Pe_p} = \frac{\varphi}{\tau} \frac{1}{Re_p Sc} + \frac{1}{2} \quad (S7)$$

Gierman suggested that when the Péclet number is larger than a certain value, which depends on the conversion ( $X$ ) and the reaction order ( $n$ ), the packed-bed reactor can be treated as plug-flow reactor (Eq. (S8)) [5, 7]. At

400 °C, the conversion of methane is 0.52 and thus the value on the right-hand side of Eq. (S8) is around 6 (assuming first-order reaction).

$$Pe > 8 n \ln\left(\frac{1}{1-X}\right) \quad (\text{S8})$$

Table S3 reports the calculated  $Pe_p$  and  $Pe$  number. The value of 61 for  $Pe$ , clearly larger than 6, suggests that the reactor is operating under plug-flow regime.

**Table S3.** Particle Péclet number,  $Pe_p$ , and Péclet number,  $Pe$ , for the catalyst packed bed of the silicon-glass reactor operating at 400 °C under 40 NmL/min of 1 % CH<sub>4</sub>/He and 4 % O<sub>2</sub>/He.

$Pe_p$	$Pe$
0.24	61 (> 6)

## External and internal mass transfer

Mears proposed a way to estimate whether external mass transfer of reacting species from the gas bulk phase to the catalyst particle surface can be neglected [3, 8]. This can be determined using Eq. (S9) which averages the contribution of the whole reactor (from inlet to outlet). In this formula ( $-r'_A$ ) is the observed reaction rate per unit of catalyst mass,  $\rho_b$  is the catalyst bulk density,  $R_p$  the catalyst particle radius,  $n$  the reaction order (here assumed to be 1),  $C_{Ab}$  the reactant concentration in the bulk phase and  $k_c$  the mass transfer coefficient. Mears proposed that when the group ( $MR$ ) in Eq. (S9) is less than 0.15, the external mass transfer can be ignored.

$$MR = \frac{(-r'_A) \rho_b R_p n}{k_c C_{Ab}} < 0.15 \quad (\text{S9})$$

The methane concentration in the bulk phase ( $C_{Ab}$ ) can be calculated from the ideal gas law (Eq. (S10)), where  $p_{CH_4}$  is the partial methane pressure (0.01 atm, 1 % in 1 atm).

$$C_{Ab} = \frac{p_{CH_4}}{RT} \quad (\text{S10})$$

The observed reaction rate ( $-r'_A$ ) times the catalyst bulk density ( $\rho_b$ ) can be determined using Eq. (S11) from the reaction rate in the main paper ( $r$ , 107 mol<sub>CH<sub>4</sub>}/mol<sub>Pd}</sub>/h), the catalyst molar amount ( $n_{cat}$ , 5.21·10<sup>-6</sup> mol) and the volume of the empty catalyst packed-bed reactor ( $V_r$ ).</sub>

$$(-r'_A) \rho_b = \frac{r n_{cat}}{V_r} \quad (\text{S11})$$

Finally, the mass transfer coefficient ( $k_c$ ) can be determined from the Sherwood number ( $Sh$ ) (Eq. (S12)) which, for very low  $Re_p$ , can be approximated according to Eq. (S13) [5].

$$Sh = \frac{k_c d_p}{D_m} \quad (S12)$$

$$Sh \approx 0.07 Re_p \quad 0.1 < Re_p < 10 \quad (S13)$$

The Mears number ( $MR$ ) can then be calculated and the result along with the external mass transfer coefficient is reported in Table S4. As evident from the  $MR$  value (0.07), clearly below 0.15, the silicon-glass microreactor is operating under no external mass transfer limitations.

**Table S4.** External mass transfer coefficient and Mears number for the silicon-glass reactor operating at 400 °C under 40 Nml/min of 1 % CH<sub>4</sub>/He and 4 % O<sub>2</sub>/He.

$k_c$ , m/s	$MR$
0.014	0.07 (< 0.15)

The Weisz Prater criterion states that for a first order reaction kinetics occurring in a spherical-shaped catalyst particle, the internal mass transfer resistance can be neglected if the dimensionless group ( $C_{WP}$ ) defined in Eq. (S14) is much smaller than 1 [3]. This, like the Mears number, averages out the reaction rate of the whole reactor (from inlet to outlet) and can also be calculated from the observed reaction rate per unit of catalyst particle mass ( $-r'_A$ ). Furthermore, one needs to know the catalyst particle density ( $\rho_c$ ), radius ( $R_p$ ), concentration of the reactant at the particle surface ( $C_{As}$ ) and the effective diffusivity ( $D_e$ ). The latter can be estimated using Eq. (S15), where  $\tau_p$  is the tortuosity,  $\varphi_p$  the porosity within the catalyst particle and  $\sigma_c$  the constriction factor. Common values for the constriction factor, tortuosity and pellet porosity are 0.8, 3.0 and 0.4, respectively [3]. Furthermore, as external mass transfer resistances can be neglected,  $C_{As}$  is assumed equal to the concentration in the bulk phase ( $C_{Ab}$ ) (Eq. (S10)).

$$C_{WP} = \frac{(-r'_A)\rho_c R_p^2}{C_{As} D_e} \ll 1 \quad (S14)$$

$$D_e = \frac{\varphi_p \sigma_c}{\tau_p} D_m \quad (S15)$$

The group  $(-r'_A)\rho_c$  can be determined using Eq. (S16), where  $(-r'_A)\rho_b$  was previously calculated in Eq. (S11) and  $\varphi$  is the catalyst bed porosity (assumed to be 0.4) [3].

$$(-r'_A)\rho_c = (-r'_A)\rho_b \frac{1}{(1 - \varphi)} \quad (S16)$$

The Weisz-Prater number ( $C_{WP}$ ) can then be calculated (Table S5). As this is much smaller than 1, the methane combustion carried in the silicon-glass microreactor used in this work is not limited by internal mass transfer resistances.

**Table S5.** Effective diffusivity and Weisz-Prater number for the silicon-glass reactor operating at 400 °C with 40 NmL/min of 1 % CH<sub>4</sub>/He and 4 % O<sub>2</sub>/He.

$D_e, \text{m}^2/\text{s}$	$C_{WP}$
$1.8 \cdot 10^{-5}$	0.003 ( $\ll 1$ )

## References

- [1] L. Kiwi-Minsker, A. Renken, in *Handbook of Heterogeneous Catalysis*, ed. G. Ertl, H. Knözinger, F. Schüth, J. Weitkamp, Wiley-VCH, Weinheim, 2nd edn, 2008, vol. 1, ch. 10, pp. 2248-2264.
- [2] E.L. Cussler, *Diffusion: Mass Transfer in Fluid Systems*, Cambridge University Press, Cambridge, 2009.
- [3] H.S. Fogler, *Elements Of Chemical Reaction Engineering*, 5<sup>th</sup> Edition, Prentice Hall, Upper Saddle River, N.J. , 2016.
- [4] J. Kestin, W. Leidenfrost, *Physica*, 1959, **25**, 537-555.
- [5] F. Kapteijn, J.A. Moulijn, in *Handbook of Heterogeneous Catalysis*, ed. G. Ertl, H. Knözinger, F. Schüth, J. Weitkamp, Wiley-VCH, Weinheim, 2nd edn, 2008, vol. 1, ch. 9, pp. 2019-2045.
- [6] J.M.P.Q. Delgado, *Heat Mass Transf.*, 2006, **42**, 279-310.
- [7] H. Gierman, *Appl. Catal.*, 1988, **43**, 277-286.
- [8] D.E. Mears, *Ind. Eng. Chem. Process. Des. Dev.*, 1971, **10**, 541-547.